Virchows Arch (1997) 430:173–180

ORIGINAL ARTICLE

Brett Delahunt · J.St. John Wakefield

Ultrastructure of streptozotocin – induced renal tumours in mice

Received: 5 June 1996 / Accepted: 17 October 1996

Abstract Streptozotocin-induced tumours in the kidneys of experimental animals have been shown to be histologically similar to human renal cell carcinoma. We report the ultrastructural features of renal tumours induced in 15 mice by a single intravenous bolus of 2.5% streptozotocin administered in a dose of 250 mg streptozotocin/kg mouse body weight. Animals were sacrificed 232–361 days after the administration of streptozotocin. On examination both kidneys from each animal contained 1–4 dysplastic tubules and 1–3 discrete tumours per kidney. Twelve dysplastic proximal convoluted tubules showing varying degrees of epthelial atypia and nine tumours exhibiting either a papillary or solid architecture were examined. Dysplastic epithelial cells and tumours of papillary and solid type exhibited complex cell borders with well-developed junctional complexes. The majority of cells contained surface microvilli, and in some cells microvilli-lined intracytoplasmic lumina were observed. Occasional dysplastic epithelial cells and tumour cells contained double-membrane vesicles 120–200 nm in diameter. These were similar to the intracytoplasmic vesicles characteristic of human chromophobe renal cell carcinoma. Intracytoplasmic collections of glycogen granules and flocculant protein were identified in both dysplastic and neoplastic cells, and where prominent they resulted in compression of cytoplasmic organelles. Coated vesicles were commonly observed. These were free within the cytoplasm and were also seen budding from strands of rough endoplasmic reticulum. The distribution of these vesicles suggested a role in protein transport from the rough endoplasmic reticulum. It is concluded that while streptozotocin-induced renal tumours have some ultrastructural features in common with human chromophobe renal cell carcinoma, the overall ultrastructural morphology differs significantly from that described for the various histological types of human renal cell carcinoma.

Key words Streptozotocin · Mouse · Renal neoplasm · Ultrastructure · Renal cell carcinoma

B. Delahunt (✉) · J.S.J. Wakefield
Department of Pathology, Wellington School of Medicine, University of Otago, PO Box 7343, Wellington South, New Zealand;
Fax: (64) 4-389 5725

Introduction

The diabetogenic antibiotic streptozotocin has a carcinogenic effect on the kidney, and in several studies the morphology of renal tumours induced by streptozotocin in rats has been shown to be similar to that of human renal cell carcinoma (RCC) [1, 5, 15, 20].

The histology of streptozotocin-induced renal tumours in mice has been characterised, and it has been suggested that the model is suitable for studies on renal carcinogenesis [10]. In a recent study the histology, morphological progression and proliferation kinetics of streptozotocin-induced murine renal tubular dysplasia and renal tumours have been described [7].

In all previous studies on the morphology of streptozotocin-induced renal tumours, observations have been confined to the light microscopic level; to date the ultrastructure of these tumours is unresolved.

This study was undertaken to determine the ultrastructure of streptozotocin-induced premalignant and malignant lesions in the mouse kidney and to compare these features with those described for human RCC in order to evaluate how appropriate the model is for studies on human renal carcinogenesis.

Materials and methods

Fifteen female CBA T6T6 strain mice aged between 30 and 96 days were used in this study, which had the approval of the Ethical Committee for Animal Experimentation of the Wellington School of Medicine. The principles of laboratory care as outlined in NIH publication 85-23 (1985) were followed.

Under light ether anaesthesia each mouse was injected intravenously via the tail vein with a single bolus of 2.5% streptozotocin

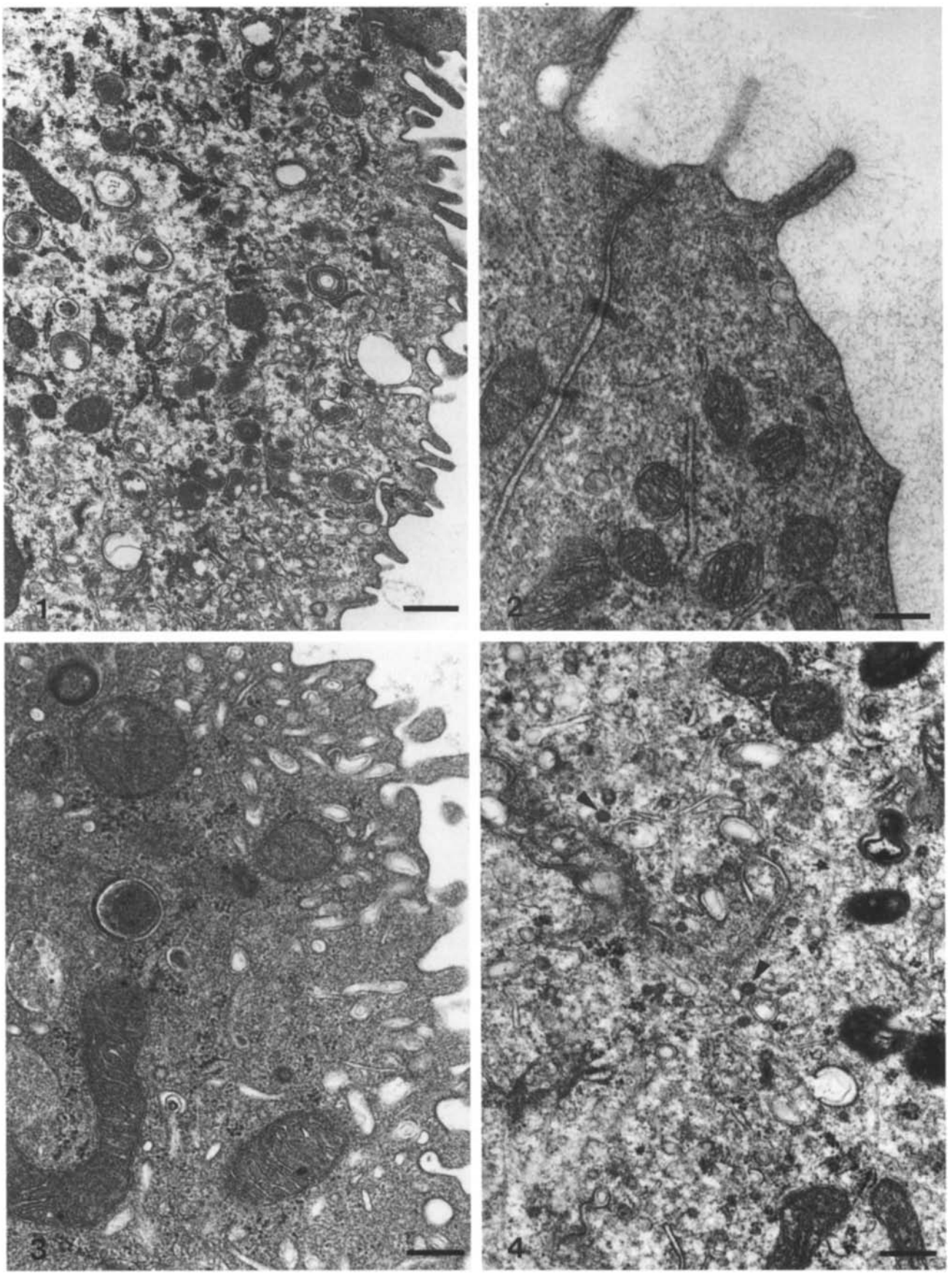
1
2
3
4

(product number S-0130, Sigma Chemical Company, St. Louis, Mo.) in 0.9% sodium chloride solution. The streptozotocin solution was prepared immediately prior to injection and was administered in a dosage of 250 mg streptozotocin per kg mouse body weight.

The animals were maintained in the Animal Facility, Wellington School of Medicine. In our previous study it was noted that beyond 32 weeks after the administration of streptozotocin, all animals sacrificed had at least one tumour in each kidney [7]. In the present study, animals were sacrificed at approximately 2-weekly intervals from day 232 to day 361 after injection. The kidneys from each mouse were dissected free and sectioned longitudinally at intervals of approximately 1 mm. Where tumours were visibly macroscopically these were selected for electron microscopic examination. In addition, several blocks were also taken from the renal cortex and medulla of each kidney.

Cubed pieces of tissue 1 mm in length were immersion-fixed in half-strength Karnovsky's fixative [13] for 1 h. The tissue blocks were then washed in a 0.2 M solution of sodium cacodylate and post-fixed for 30 min in 1% osmium tetroxide, before being dehydrated in a graded series of alcohols and two changes of propylene oxide. The tissue was embedded in Epon 812, which was polymerised for 24 h at 60° C. Sections 1 μm thick were cut and stained with toluidine blue for light microscopic examination. Thin sections, stained with uranyl acetate and lead citrate, were examined with a Siemens 102 electron microscope at 80 kV.

Results

Twelve dysplastic proximal convoluted tubules and nine renal tumours from different animals were available for ultrastructural examination. The tumours exhibited either a papillary (four tumours) or a solid architecture (five tumours).

Light microscopic examination of the renal tumours showed them to have a morphological appearance similar to that of human RCC, being derived from renal tubular epithelium and consisting predominantly of cells containing a granular cytoplasm with varying degrees of cytoplasmic vacuolation. The detailed histological findings and proliferation kinetics of streptozotocin-induced renal tubular dysplasia and renal tumours in mice have been reported elsewhere [7].

The tumour cells were markedly pleomorphic, and apart from the distribution of microvilli there was no consistent feature in the ultrastructure of dysplasic epithelial cells, papillary outgrowths of neoplastic cells or solid tumours. Microvilli were present on the luminal surface of cells and were numerous in dysplastic and papillary neoplastic foci (Fig. 1), being less frequently observed in those solid tumours in which a luminal surface could still be identified. A luxuriant glycocalyx was often present on the microvilli (Fig. 2), a feature not seen in normal non-neoplastic tubules.

Where microvilli were numerous, coated pits and invaginations at the base between microvilli were seen (Fig. 3) and coated vesicles were commonly found in the peripheral cytoplasm (Fig. 4). In places these vesicles were attached to short strands of rough endoplasmic reticulum (Fig. 5).

The luminal cytoplasm of some superficial cells contained double-membrane profiles (Figs. 6, 7), which were infrequently seen in other areas of the tumours. These were usually vesicular, although less commonly elongate, c-shaped or irregular profiles were identified. The majority of these structures measured 120–200 nm in cross-sectional diameter although occasional elongate forms up to 400 nm in length were seen. The membrane of these vesicles had a unit structure, although in many cases the inner membrane was not easily resolved.

A variety of membrane-bound secretory or lysosomal bodies were present within the cytoplasm of tumour cells. These occurred in a patchy distribution, with a few cells having large numbers, while in most cells few or none of these bodies were seen. Two types of secretory or lysosomal bodies were identified. The first of these was generally small and variable in shape, ranging from spherical to elongate or comma-shaped in profile, and exhibited an extremely electron-dense content (Fig. 8). These also frequently contained clear areas and were most often found in the deeper central cells of solid tumours. The other membrane-bound body was typically lysosomal in appearance, being variable in shape and size, with an heterogeneous content ranging from strongly electron-dense areas to clear areas which, on occasion, contained myelin figures (Fig. 9).

In some cells irregular-shaped non-membrane-bound patches were seen. In these areas the patches contained particles having the appearance of flocculant protein and glycogen granules in the non-aggregated or β form [22] (Figs. 10, 11). In most areas the granules had the size and form of glycogen although few of the granules stained as strongly as did the glycogen situated in the immediately adjacent cytoplasm. The majority of granules stained weakly, giving the areas an electron-lucent appearance. The extent of these areas, from small foci up to extensive deposits, excluded all organelles in the cell apart from the nucleus. Cells with extensive areas of granules that occupied most of the cell tended to occur in clusters.

In a few cells intracytoplasmic lumina were present with diameters up to 10 μm across. These contained diffuse proteinaceous material with cytoplasmic microvilli projecting into the vesicle (Fig. 12).

Cell borders were focally complex, being composed of infolded cytoplasmic processes. Junctional complexes were frequently seen and were most often situated toward the luminal surface of cells (Fig. 10).

Tubules with a normal histological appearance exhibited occasional ultrastructural changes. Some cells had reduced numbers of microvilli and basal membrane in-

◀ **Fig. 1** Segment of a cell from a papillary renal tumour; microvilli are present on the luminal surface. ×20,000, *bar* 0.5 μm

Fig. 2 Luminal region of 2 cells from a papillary renal tumour with a prominent glycocalyx. ×52,000, *bar* 0.2 μm

Fig. 3 Part of a cell from a papillary renal tumour; coated pits are present between microvilli. ×52,000, *bar* 0.2 μm

Fig. 4 Part of a cell from a papillary renal tumour; coated vesicles (*arrowheads*) are common in the tumour cell cytoplasm. ×40,000, *bar* 0.2 mm


5

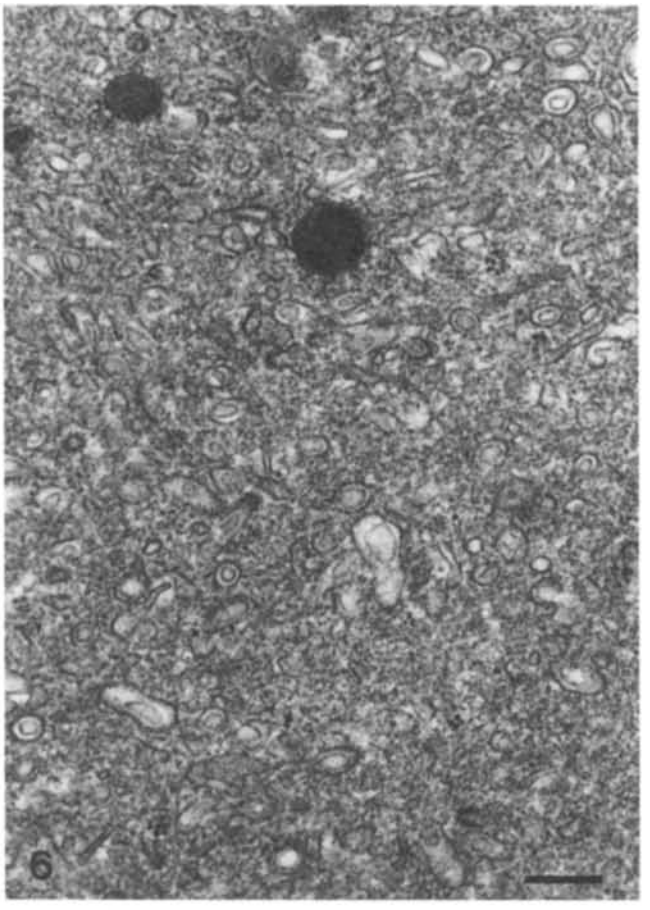
6

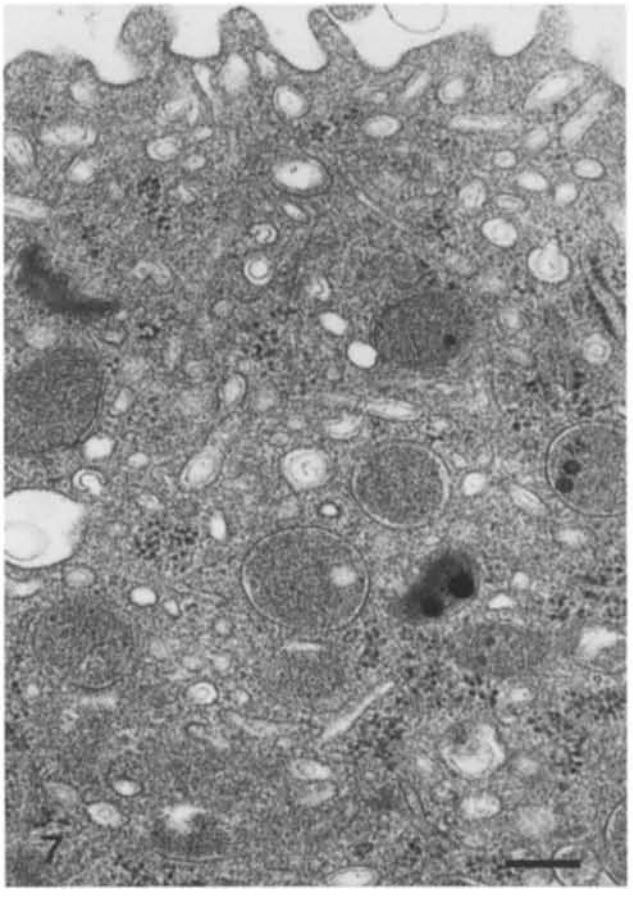
7

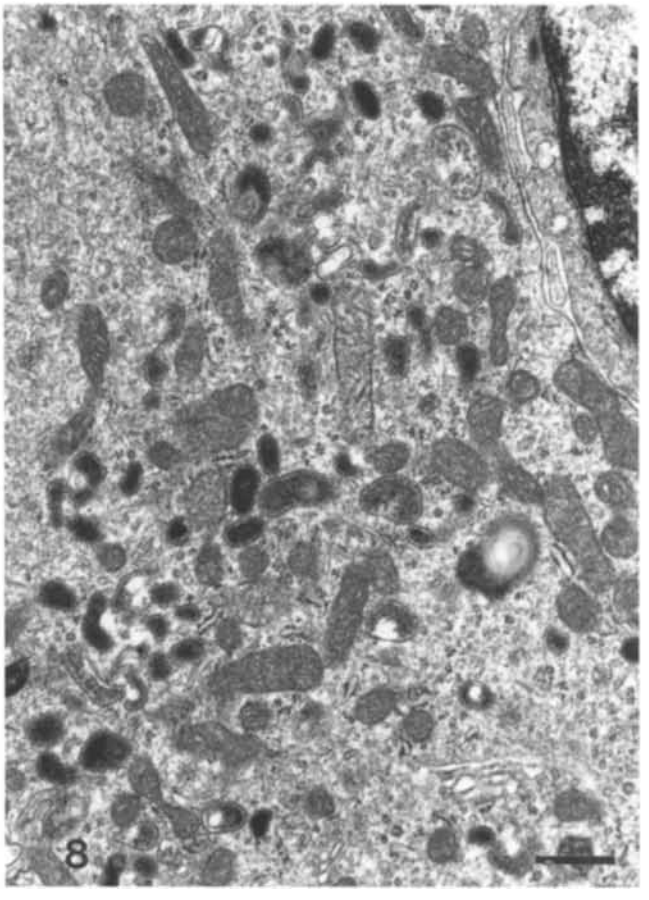
8

vaginations. The most striking change was the accumulation of glycogen identical to that seen in neoplastic cells.

Discussion

Examination of tumour fine structure showed streptozotocin-induced renal tumours in mice to have a number of ultrastructural features similar to those observed in human RCC.

Both papillary and solid tumours induced by streptozotocin were found to have surface microvilli. This feature was prominent in papillary tumours, being most frequently seen on the surface of cells adjacent to tumour lumina. The presence of microvilli has been previously noted in both granular cell and clear cell variants of RCC [8, 25, 27], and this feature has been considered as evidence that these tumours are derived from renal proximal convoluted tubule cells [27]. Large intracytoplasmic vesicles lined with microvilli have been noted in the present study. These have also been observed in human clear cell RCC and small tubular renal "adenomas" [12, 17, 18, 25], and in animal models of renal neoplasia induced by dimethylnitrosamine, lead and cycasin [11, 14] in addition to spontaneous renal tumours in rats [24]. Like surface microvilli, intracytoplasmic microvilli-lined vesicles are most frequently seen in human RCC of the granular cell type [27].

The formation of pinocytotic vesicles by invagination of the cell membrane between microvilli has been recorded in human clear cell RCC [27]. In the present study abundant coated vesicles were seen within the tumour cell cytoplasm, being predominantly situated towards the luminal surface of the cell, and coated pits were commonly encountered along the luminal plasma membrane. It was originally assumed that the majority of coated vesicles originated from invagination of these pits, as this is the route by which a variety of specific components are taken into a cell [19]. This interpretation was complicated by the finding of coated vesicles attached to the cisternae of rough endoplasmic reticulum. Although this is an unusual association, coated vesicles have previously been reported budding from rough endoplasmic reticulum [23]. In cultured CHO cells infected by vesicular stomatitis virus, the viral G protein manufactured in the endoplasmic reticulum of infected cells is transferred to the Golgi apparatus by coated vesicles, prior to export from the cell [23]. The association between coated vesicles and rough endoplasmic reticulum in mouse tumour cells suggests that at least some of the coated vesicles in the peripheral cytoplasm are transporting protein for export from the endoplasmic reticulum.

A striking feature identified in this series of streptozotocin-induced murine tumours was the numerous double-membrane vesicles identified within the tumour cell cytoplasm. These vesicles, which were variable in shape, bore a resemblance to the microvesicles described from studies on the cytoplasm of a variant of RCC first described in nitrosomopholine-induced renal tumours in the rat and later identified in series of human RCC [3, 28]. These tumours, designated chromophobe RCC, contain cytoplasmic microvesicles 150–300 nm in diameter that consist of a closed, smooth membrane and are round to elongate in shape. These contain occasional internal membrane-lined vesicles, possibly formed by invagination of the outer membrane, that incorporate cytoplasmic ground substance or electron-dense glycogen-like granules [29, 30].

Light microscopic examination of the tumours in the present study has shown the presence of clear cytoplasm in neoplastic cells that, in rare instances, is seen in almost all the cells within individual tumours. These clear cells bear a superficial resemblance to clear cells and chromophobe cells of human RCC. In some tumours these clear areas appear as foci of vacuolation, being confined to the basal portion of the cell and compressing luminal granular cytoplasm. Ultrastructural studies show these areas to consist of aggregates of granules resembling monoparticulate glycogen that exhibit varying density of staining. Brummer and Rabes [6] reported the presence of glycogen within vacuolated cells of dimethylnitrosamine-induced tumours in rat kidneys. In these tumours the glycogen was diffusely dispersed throughout the tumour cytoplasm and was unrelated to observed areas of vacuolation. The vacuoles were frequently multiple within individual cells, imparting a reticular pattern to the tumour cell cytoplasm, and were thought to be the product of fat deposition. Intracytoplasmic glycogen has not been reported in chromophobe cell renal tumours induced in the rat by lead or *N*-nitrosodiethylamine [16], while only scanty, diffusely scattered glycogen is seen on electron microscopic examination of dimethylnitrosamine-induced renal adenocarcinoma in the rat [11].

Tubular glycogenosis has been noted in rats following treatment with nitrosomorpholine [2]. In these animals clear cell tumours were observed 22 weeks after oral administration of nitrosomorpholine, and on ultrastructural examination the tumours were found to contain intracytoplasmic glycogen and lipid. In addition, mucopolysaccharides were found within tumour interstitial cells. The diverse nature of these intracytoplasmic aggregates was thought to reflect a disturbance of cell metabolism associated with renal tubule cell carcinogenesis. Although scattered aggregates of glycogen have been described in the cytoplasm of human chromophobe RCC, extensive deposits have not been observed [29, 30]. Intracytoplas-

◀ **Fig. 5** A composite micrograph of parts of three cells (*top* and *middle*) from papillary renal tumours and (*bottom*) from a solid tumour showing coated vesicles attached to endoplasmic reticulum. ×80,000, *bar* 0.2 μm

Fig. 6 Part of a cell from a solid renal tumour; numerous membrane-bound vesicles are present. ×50,000, *bar* 2 μm

Fig. 7 Part of a cell from a papillary renal tumour; membrane-bound vesicles are present towards the luminal surface. ×52,000, *bar* 0.2 μm

Fig. 8 Part of a cell from a solid renal tumour; electron-dense bodies are common. ×19,000, *bar* 0.5 μm


9

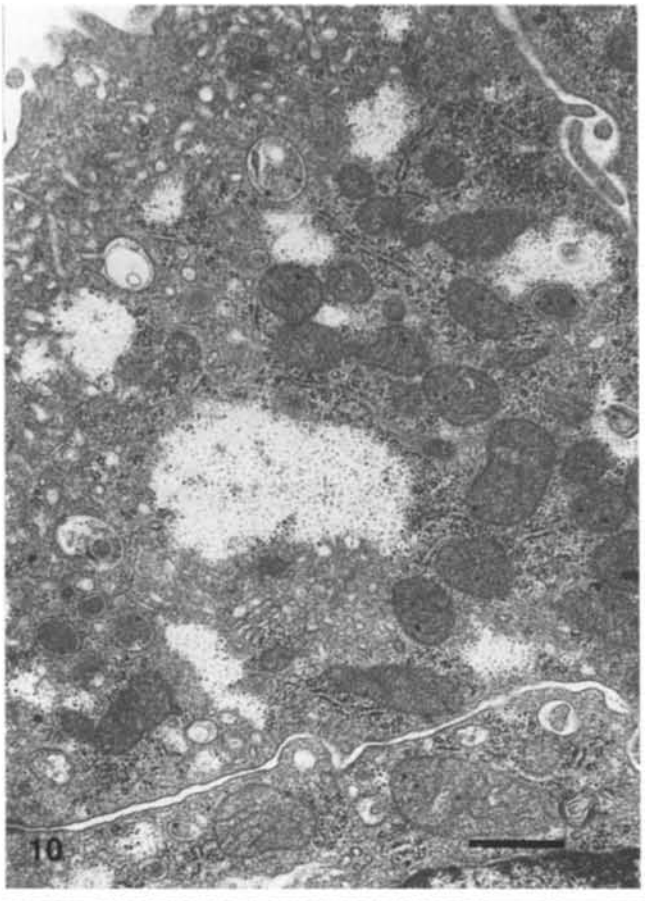
10

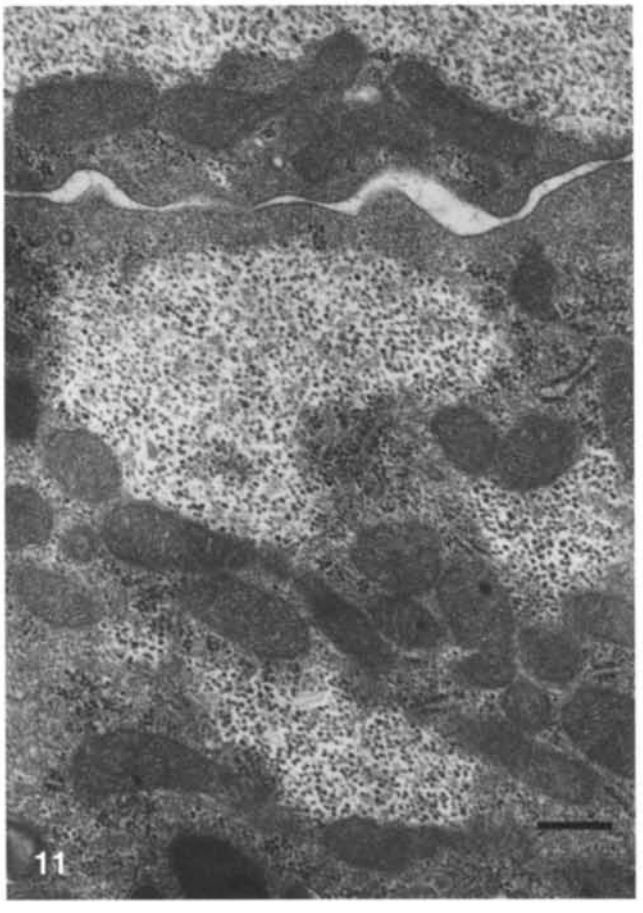
11

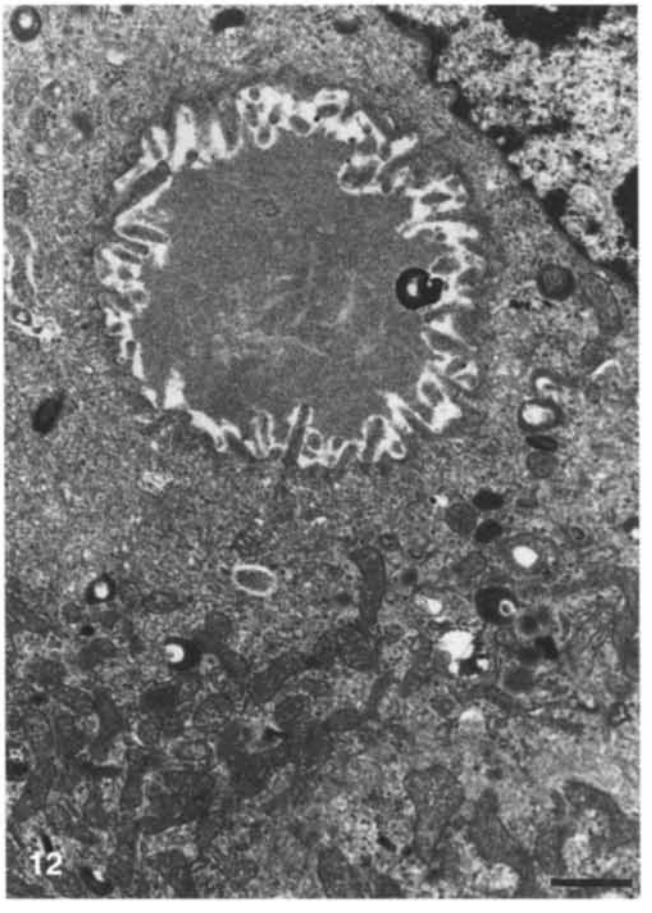
12

mic glycogen is a feature of human clear cell RCC and is accompanied by abundant lipid droplets [26]. In human clear cell RCC, the glycogen is dispersed throughout the cytoplasm of the tumour cell rather having a localised distribution that results in compression of cytoplasmic organelles and the nucleus [9].

Ultrastructural studies of normal human kidneys have shown intracytoplasmic glycogen within cells of the middle portion of the proximal convoluted tubule [4]. Glycogen is also abundant in cells of the distal convoluted tubule in hyperglycaemic patients with diabetes mellitus, and in one report the degree of glycogen deposition was correlated with the severity of the hyperglycaemic state [4]. Similar features have been described from the kidneys of rats treated with streptozotocin, where glycogenosis was observed in the tubules of the outer renal cortex and the outer stripe of the outer medulla [21]. In the present series of tumours similar vacuolation of epithelial cells was identified in tubules within the renal cortex [7], and this is likely to be the result of hyperglycaemia associated with streptozotocin-induced diabetes.

The areas of vacuolation identified within renal tumours in this study are similar to hyperglycaemia-induced tubular vacuolation reported from human kidneys [4]. They are also similar to vacuoles seen at both the light microscopic and electron microscopic levels in the convoluted tubules of various experimental animals treated with streptozotocin, but do not have morphological counterparts in either human clear cell or chromophobe RCC. These vacuoles may result from altered tumour cell metabolism similar to that postulated for the nitrosomorpholine rat tumour model [2], or may be the product of glycogen deposition associated with streptozotocin-induced diabetes. These vacuoles may therefore represent abnormal glycogen metabolism in well-differentiated tumour cells that have retained the ability to store glycogen in a manner similar to non-neoplastic tubular epithelium.

This study has shown streptozotocin-induced renal tumours in mice to have some ultrastructural features in common with human RCC and, in particular, with the chromophobe variant of RCC. The presence of abundant aggregates of intracytoplasmic glycogen and the unusual relationship between coated vesicles and rough endoplasmic reticulum has not been recorded for human RCC, and these findings suggest that this model may not be fully applicable to human tumours.

◀ **Fig. 9** Parts of two cells from a solid renal tumour; several heterogeneous lysosomes are present. ×22,000, *bar* 0.5 μm

Fig. 10 Parts of three cells from a papillary tumour; scattered electron-lucent areas containing granular deposits (glycogen) are present. ×25,000, *bar* 0.5 μm

Fig. 11 Parts of two cells from a solid renal tumour with aggregates of glycogen and flocculant protein. ×43,000, *bar* 0.25 μm

Fig. 12 Part of a cell from a solid renal tumour with a large intracytoplasmic lumen containing microvilli. ×10,000, *bar* 1 μm

Acknowledgements This study was funded by a grant from the W.J. and A.A. Morris Cancer Research Foundation whose assistance is gratefully acknowledged.

References

1. Arison RN, Feudale EL (1967) Induction of renal tumour by streptozotocin in rats. Nature 214:1254–1255
2. Bannasch P, Krech R, Zerban H (1978) Morphogenese und Mikromorphologie epithelialer Nierentumoren bei Nitrosomopholin-vergifteten Ratten. II. Tubuläre Glykogenose und die Genese von klar- oder acidophilzelligen Tumoren. Z Krebforsch Klin Onkol 92:63–86
3. Bannasch P, Krech R, Zerban H (1980) Morphogenese and Mikromorphologie epithelialer Nierentumoren bei Nitrosomorpholin-vergifteten Ratten. IV. Tubuläre Läsionen und basophile Tumoren. J Cancer Res Clin Oncol 98:243–265
4. Biava C, Grossman A, West M (1966) Ultrastructural observations on renal glycogen in normal and pathologic human kidneys. Lab Invest 15:330–356
5. Bleasel AF, Yong LCJ (1982) Streptozotocin-induced diabetic nephropathy and renal tumors in the rat. Experientia 38:129–130
6. Brummer C, Rabes HM (1992) Morphology and proliferation kinetics of early tumour stages induced by dimethylnitrosamine in rat kidneys. Virchows Arch [B] 62:133–142
7. Delahunt B, Cartwright PR, Thornton A, Dady PJ (1995) Proliferation kinetics of streptozotocin-induced renal tumours in mice. Virchows Arch 425:577–582
8. Ericsson JLE, Seljelid R, Orrenius S (1966) Comparative light and electron microscopic observations of the cytoplasmic matrix in renal carcinoma. Virchows Arch [A] 341:204–223
9. Fisher ER, Horvat B (1972) Comparative ultrastructural study of so-called renal adenoma and carcinoma. J Urol 108:382–386
10. Hard GC (1985) Identification of a high-frequency model for renal carcinoma by the induction of renal tumors in the mouse with a single dose of streptozotocin. Cancer Res 45:703–708
11. Hard GC, Butler WH (1971) Ultrastructural aspects of renal adenocarcinoma induced in the rat by dimethylnitrosamine. Cancer Res 31:366–372
12. Holm-Nielsen P, Olsen TS (1988) Ultrastructure of renal adenoma. Ultrastruct Pathol 12:27–39
13. Karnovsky MJ (1965) A formaldehyde-glutaraldehyde fixative of high osmolality for use in electron microscopy. J Cell Biol 27:137A–138A
14. Mao P, Molnar JJ (1967) The fine structure and histochemistry of lead-induced renal tumors in rats. Am J Pathol 50:571–603
15. Mauer SM, Lee SL, Najarian JS, Brown DM (1974) Induction of malignant kidney tumors in rats with streptozotocin. Cancer Res 34:158–160
16. Nogueira E (1987) Rat renal carcinogenesis after chronic simultaneous exposure to lead acetate and *N*-nitrosodiethylamine. Virchows Arch [B] 53:365–374
17. Oberling C, Rivière M, Haguenau F (1960) Ultrastructure of the clear cells in renal carcinomas and its importance for the determination of their renal origin. Nature 186:402–403
18. Okada Y, Yokoyama M, Tokue A, Takayasu H (1969) Ultrastruture of renal cell carcinoma. Urologia (Treviso) 36:11–19
19. Pearse BMF, Robinson MS (1990) Clathrin adaptors and sorting. Annu Rev Cell Biol 6:151–171
20. Rakieten N, Gordon BS, Cooney DA, Davis RD, Schein PS (1968) Renal tumorigenic action of streptozotocin (NSC-85998) in rats. Cancer Chemother Rep 52:563–567
21. Rasch R (1984) Tubular lesions in streptozotocin-diabetic rats. Diabetologia 27:32–37
22. Revel JP (1964) Electron microscopy of glycogen. J Histochem Cytochem 12:104–114
23. Rothman JE, Fine RE (1980) Coated vesicles transport newly synthesized membrane glycoproteins from endoplasmic reticulum to plasma membrane in two successive stages. Proc Natl Acad Sci USA 77:780–784

24. Seljelid R (1966) An electron microscopic study of the formation of cytosomes in a rat kidney adenoma. J Ultrastruct Res 16:569–583
25. Seljelid R, Ericcsson JLE (1965) Electron microscopic observation on specialisations of the cell surface in renal clear cell carcinoma. Lab Invest 14:435–447
26. Sun CK, Bissada NK, White HJ, Redman JF (1977) Spectrum of ultrastructural patterns of renal cell adenocarcinoma. Urology 9:195–200
27. Tannenbaum M (1971) Ultrastructural pathology of human renal cell tumors. In: Sommers EC (ed) Pathology annual, vol 6. Apple-Century-Crofts, New York, pp 249–277
28. Thoenes W, Störkel S, Rumpelt HJ (1985) Human chromophobe cell renal cell carcinoma. Virchows Arch [B] 48:207–217
29. Thoenes W, Störkel S, Rumpelt HJ (1986) Histopathology and classification of renal tumors (adenomas, oncocytomas and carcinomas). Pathol Res Pract 181:125–143
30. Thoenes W, Störkel S, Rumpelt HJ, Moll R, Baum HP, Werner S (1988) Chromophobe cell renal cell carcinoma and its variants – a report on 32 cases. J Pathol (Lond) 155:277–287